Properties of Hydrophobic Polymer Melts Tethered to the Water Surface As Determined with in Situ X-ray Reflectivity

Hubert Baltes,[†] Michael Schwendler,[†] Christiane A. Helm,[†,‡] Robert Heger,[§] and Werner A. Goedel*[,§]

Institut für Physikalische Chemie, Johannes Gutenberg-Universität Mainz, Jakob-Welder Weg 11, 55099 Mainz, Germany, Fachrichtung Strukturforschung, Universität des Saarlandes, Postfach 151150, 66041 Saarbrücken, Germany, and Max-Planck Institut für Kolloid- & Grenzflächenforschung, Haus 9.9, Rudower Chaussee 5, 12489 Berlin, Germany

Received February 19, 1997; Revised Manuscript Received July 2, 1997[⊗]

ABSTRACT: Insoluble monolayers of hydrophobic polymers with low glass transition temperature (perfluoropolyethers, polyisoprenes) and a single ionic head group (carboxylic acid, sulfonate) have been characterized at the air/water interface via X-ray reflectivity measurements. The films are considerably thicker (30−420 Å) than conventional Langmuir monolayers of low molecular weight substances or polymers with surface active repeat units. The thickness is inversely proportional to the area per head group and is in accordance with a model assuming a solvent-free hydrophobic layer of the same density as the bulk material.

Introduction

Polymers with suitable head groups can bind to a surface specifically with the head group. If the lateral distance between the head groups is considerably shorter than the dimensions of the undisturbed polymer coil, the polymers form a continuous film; the so-called "brush" and neighboring chains interact with each other. In general, we have to distinguish two cases: a polymer brush in contact with a good solvent ("swollen brush"; cf. Figure 1a) and a solvent free brush of a polymer melt ("solvent free brush", "melt brush", or "dense brush"; cf. Figure 1b). In the first case the brush is swollen with solvent and the interaction between chains is primarily osmotic.[1−3] In the latter case there is no solvent to fill voids in between polymer segments, and it seems reasonable to assume that the density of polymer segments in the brush is the same as in the bulk of the free homopolymer and that the total volume or three-dimensional density of the brush is constant.

Theories on dense polymer brushes usually assume this constant volume of the polymer layer.[4,5] They focus mainly on the prediction of the complex morphologies of phase-separated block copolymers, which can be constructed from polymer brushes by linking the head groups of incompatible chains (cf. Figure 1c). However, they can as well be applied to monolayers of a solvent-free polymer brush, and their validity can be demonstrated, as will be shown directly in this paper.

One can expect "dense brush" monolayers to be considerably thicker than monolayers of low molecular weight substances. They may therefore be of interest in certain applications like electrical insulation or lubrication, when a thickness of more than 10 nm is desirable. In addition, the assumption of constant volume of the brush implies that the thickness is inversely proportional to the area per head group and is proportional to the chain length. One might therefore be able to fine tune the thickness of these monolayers just by variation of the area per head group.

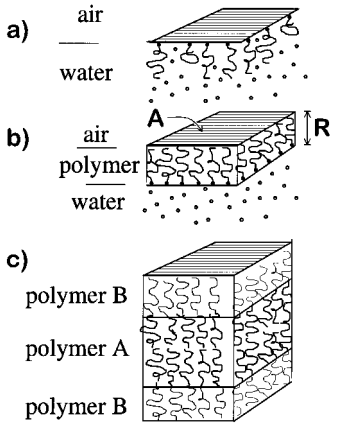

Figure 1. Schematic drawing of polymer brushes in different surroundings. (a) A hydrophylic polymer brush anchored at the air/water interface is swollen due to the polymer immersion into the aqueous phase. (b) A hydrophobic brush anchored at the air/water interface is solvent free; it is a "melt brush" or a "dense brush". (c) The morphologies of phase-separated block copolymers are calculated; assuming two incompatible solvent-free linked polymer chains, both polymer phases are described as "melt brushes".

Hydrophobic polymers with polar groups have been applied onto the water surface in a Langmuir trough. It has been shown that they form continuous films on the water surface and give rise to reproducible and reversible isotherms[6,7] which—if the chain is longer than 300 σ-bonds—are dominated by the entropy change due to the stretching of the polymer chains upon lateral compression.[8] Polymer monolayers on the water surface can be transferred onto solid substrates via the Langmuir−Blodgett technique,[9] and the transferred thin layers exhibit some interesting properties: in certain cases they can be degraded to form nanometer-thick mechanically stable inorganic coatings,[10] and they may even retain their biofunctionality if exposed to air.[11]

Attempts have been made to measure the thickness of dense brushes transferred onto solid substrates via Langmuir−Blodgett transfer.[7,8] Yet, the thickness of these films changes within weeks. Since there is no easy method to determine the location of the head groups in the layer, one cannot exclude the possibility that the head groups leave the interface shortly after transfer. Preliminary AFM measurements even suggest

* To whom correspondence should be addressed. E-mail: goedel@mpikg.fta-berlin.de.
[†] Johannes Gutenberg-Universität Mainz.
[‡] Universität des Saarlandes.
[§] Max-Planck Institut für Kolloid- & Grenzflächenforschung.
[⊗] Abstract published in *Advance ACS Abstracts,* September 15, 1997.

S0024-9297(97)00232-5 CCC: $14.00 © 1997 American Chemical Society

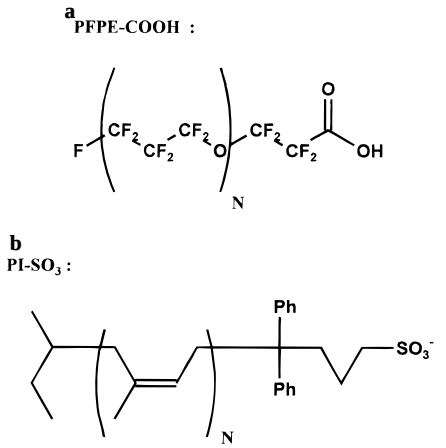

Figure 2. Chemical formulas of the polymers used. In case of PFPE−COOH, the mean number of repeat units, N, is 22, the various PI−SO_3-N are listed in Table 1. A repeat unit of PFPE has 80 electrons; one of PI−SO_3-N has 36 electrons. Thus, the PFPE−COOH provides a much higher contrast.

Table 1. Polymers Used in This Work, as Well as the Number of Repeat Units and the Polydispersity

name	head group	ρ_m (kg/m^3)	M_n (g/mol)	M_w/M_n	N
perfluoropoly(oxypropylene) PFPE−COOH	−COOH	1800	3800	–	22
polyisoprene PI−SO_3-140	−SO_3^-	913	9638	1.14	140
PI−SO_3-538	−SO_3^-	913	45900	1.02	538
PI−SO_3-810	−SO_3^-	913	55020	1.02	810

that films transferred onto mica dewet. If, however, the film is tethered to the water surface of a Langmuir trough, one can measure the film pressure while performing the reflectivity experiments and thus make sure that the majority of the head groups remain at the interface during the measurement. After the X-ray experiment the reversibility of the isotherm can be checked.

In this paper we characterize films of hydrophobic polymers with polar head groups at the air/water interface using X-ray reflectivity measurements.[12,13] The main advantage of investigating polymer brushes at the fluid/gas interface is the easy control of the anchoring density which can be varied by a factor of 2 via compression of the surface with a movable barrier. X-ray reflectivity is especially suitable to verify the assumption of the constant volume of the brush: the index of refraction is directly proportional to the electron density, which in turn is inversly proportional to the volume occupied by the polymer. The volume per monomer unit is directly calculated from the electron density and compared with the well-known value measured in the bulk phase. While the electron density of the polymers is deduced from the contrast of the X-ray reflectivity measurements, the film thickness is deduced from the interference maxima and minima. From the product of film thickness and area per head group, the volume per monomer unit is calculated again. One should obtain the same result by these two methods.

Materials and Methods

Linear perfluoropolyether (PFPE−COOH, trade name Demnum-SH) with one CF_3 group at one end and a COOH group on the other end of the chain (see Figure 2a and Table 1) was obtained from Daikin Ltd. and used as received. The polymer contained approximately 30% of perfluoropolyoxypropylene chains with CF_3 groups on both ends.

Linear polyisoprenes (PI−SO_3) with a *sec*-butyl group at one end and a sulfonate group at the other end (see Figure 2b) have been prepared via anionic polymerization followed by reaction with diphenylethylene and propanesultone. The characterization of the polymers is summarized in Table 1. A general description of the synthesis and characterization is given in ref 8.

Perfluoreohexane (Aldrich), trichloromethane (Aldrich 99.99% pure), and ethanol (Aldrich 99.99% pure) were used as received. Water (resistivity 18 MΩ/cm) was purified with an ion exchange/filter system (Millipore).

Isotherms on the surface of pure water were recorded using a rectangular Langmuir trough made of poly(tetrafluoroethylene), equipped with one barrier and a Wilhelmy plate system for the detection of surface pressure (Riegler & Kirstein, Wiesbaden, Germany). The perfluoropolyether was spread from solutions in perfluorohexane, the polyisoprenes were spread from chloroform solutions which contained 0.05 wt % of polymer and 10 wt % of ethanol.

All isotherms were recorded at room temperature. The number average molecular weight was used to calculate the mean area per molecule of the polymers.

Specular X-ray reflectivity measurements were performed with a home-built θ/θ instrument as described in ref 14. We used a Langmuir trough in a He-filled enclosure with X-ray transparent Capton windows. The trough is placed on an active vibration isolation system. A conventional Cu anode (λ=1.54 Å, 40 kV, 55 mA) with a line focus serves as the source. For good angular resolution, the slits adjacent to the tube and the secondary monochromator are set to $s_1 = s_4 = 200$ μm, with the slits before and after the Langmuir trough set to $s_2 = s_3 = 100$ μm. The distance between source and detector is 1.5 m. With this setup the incident intensity was about 7×10^6 counts/s.

Data Analysis

Specular reflection of X-rays gives information on the electron-density variation (scattering-density-length variation) in the direction perpendicular to the surface with Å-resolution.[12] For X-rays with a wavelength of $\lambda \approx 1.5$ Å, the index of refraction n for low atomic weight materials depends only on the electron-density ρ and experimental constants (r_o is the Thomson radius of an electron):

$$n = 1 - \frac{r_o}{2\pi}\rho\lambda^2 \tag{1}$$

The refractive index deviates by only aproximately 10^{-5} from 1; therefore dynamic effects (i. e. multiple scattering) or beam refraction contribute to the reflectivity R only at incident angles lower than two or three critical angles. Thus, the reflectivity may be seen as the Fresnel reflectivity R_F of the bulk phase (calculated for an infinitely sharp interface) modulated by interference effects from the thin surface layer. This leads to the kinematic approximation[12]

$$\frac{R}{R_F} = \frac{1}{\rho_w{}^2}\left|\int \rho'(z) e^{iQz}\, dz\right|^2 \tag{2}$$

where ρ_w is the electron density of the bulk phase (water, $\rho_w = 0.333$ e$^-$/Å^3), $\rho'(z)$ is the gradient of the electron density along the surface normal, z is the direction perpendicular to the interface and Q is the normal wavevector transfer.

To model the electron density profile of the thin film, the monolayer is subdivided into slabs (the popular "box model"). Each box is parametrized by a length and an electron density; also, smearing parameters are necessary to describe the interfacial roughness.[13] These

models are especially convenient if one wants to quantify changes of the monolayer structure with a variation of the external parameters. For each measurement, the numerical values of the parameters are determined by least-square methods.[15]

If the anchoring group is neglected, the polymer may be described as a slab of homogeneous thickness. Then, the integration of eq 2 yields

$$\frac{R}{R_F} = [\rho^2 e^{-Q^2\sigma_{PA}^2} + (\rho - \rho_w)^2 e^{-Q^2\sigma_{PW}^2} + 2\rho(\rho - \rho_w) e^{-Q^2(\sigma_{PW}^2 + \sigma_{PA}^2)/2} \cos(Qd)]/\rho_w^2 \quad (2a)$$

with ρ as the electron density of the polymer film, d its thickness, and σ_{PW} (σ_{PA}) the roughness of the polymer/water (polymer/air) interface, respectively. Basically, the first two terms with the prefactors ρ^2/ρ_w^2 and $(\rho - \rho_w)^2/\rho_w^2$ describe the contrast in comparison to a clean water surface, where the prefactor would be just 1. The last term with the prefactor $2(\rho/\rho_w)(\rho - \rho_w)/\rho_w$is an interference term, whose period is determined by the film thickness d.

For the derivation of eqs 2 and 2a, dynamic effects and beam refraction were neglected. To obtain the optimum description of the data, the actual calculation was done using the dynamical approach as described in ref 16.

Results and Discussion

We shall describe first the results obtained with PFPE, than those with PI−SO_3. In the inset of Figure 3 the isotherm of PFPE is given. Between the onset of pressure and collapse we expect the film to be homogeneous. In this regime, the area per head group can be varied by a factor of 2. The reflectivity curves measured along the isotherm are given in Figure 3 as function of the vertical wavevector transfer Q. All reflectivity measurements are normalized with respect to the Fresnel reflectivity R_F.

The reflectivity curves are rather structured. Already at the highest molecular area, where the film is thinnest, two maxima and one minimum can be distinguished. On compression, the first maximum shifts to lower Q values, and the extrema get closer, both obvious indications of an increase in film thickness. This is visualized by the dotted lines in Figure 3, which connect the minima of the same order. At the highest anchoring density, four maxima and three minima are observed. It is rather remarkable that the minima are always equidistant, a feature which is typical for a homogeneous film without lateral or vertical structure as described in eq 2a. The only obvious deviations from the simple model occur at the first maximum of reflectivity curves measured at high molecular areas. This may be caused by vertical and/or lateral inhomogeneities. Yet these deviations are too small and irregular to describe them with a consistent model for all measurements.

Another common property of all reflectivity curves is the constant and extremely high contrast, note that the first maximum always occurs at $\approx 3.5R/R_F$. The unchanging contrast has to be due to a constant electron density of the film, which appears to be independent of the lateral film compression. Thus we have already a qualitative indication that the assumption of constant volume is correct.

For a quantitative determination of the electron density, simulations have to be performed. To obtain a description of the data, one has to accommodate both the intensity decrease of the maxima with increasing order as well as the decreasing contrast of higher order extrema. Therefore, two roughnesses are introduced, one describing the polymer/water interface σ_{PW}, the other the polymer/air interface σ_{PA}.

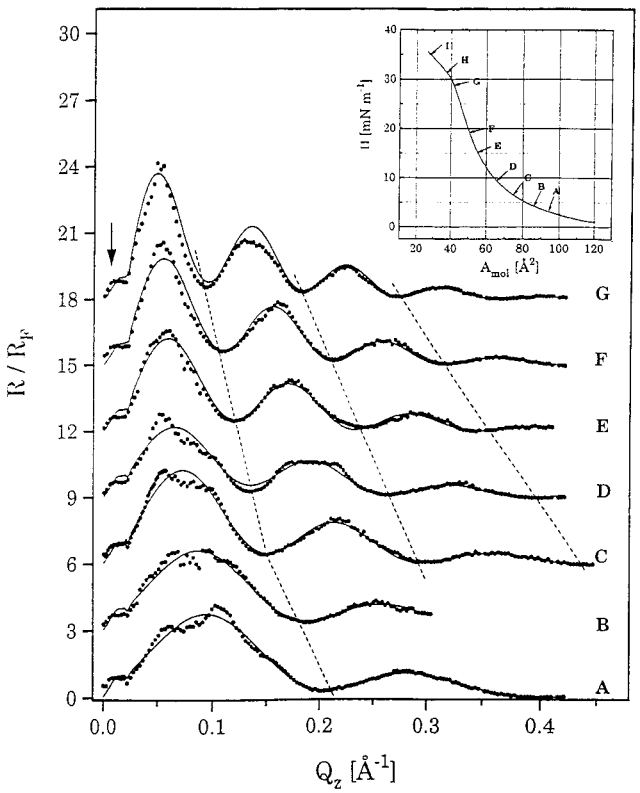

Figure 3. Normalized X-ray reflectivity of a PFPE−COOH monolayer on water at the molecular areas indicated at the isotherm in the inset. The measured X-ray intensities are given together with their statistical error bars; the solid lines are simulations with the optimized parameters given in Table 2. For clarity, each measurement is vertically displaced by 3 units from the next. The interference minima of the same order are connected with dotted lines.

The best simulation for each measurement (full lines) is shown in Figure 3 together with the experimental data. The optimum parameters are listed in Table 2. The parameter error is estimated rather conservatively: the parameter under question is changed until χ^2 increases by 30%, while all the other parameters are allowed to readjust. As can be seen in Figure 3, curves with up to nine extrema can be satisfactorily described with only four adjustable parameters. This is a strong argument for the validity of the one-slab model describing a homogeneous layer without internal structure.

As Table 2 demonstrates, the tethered polymer layer shows in principle the expected behavior: On compression the film thickness doubles from ~30 to ~70 Å, while the area per head group is halved, from 93.4 to 44.2 Å^2. The electron density is constant within the error and amounts to $\rho = 0.5057 \pm 0.020$ e$^-$/Å^3. The electron density of the film is much higher than the one of water, $\rho_w = 0.333$ e$^-$/Å^3.

The parameter with the highest error is the roughness describing the polymer/water interface, $\sigma_{PW} = 2.8 \pm 2$ Å. Note that the physical meaning of the parameter σ_{PW} is somewhat ambiguous. It describes the dynamical roughness caused by vertical movement in the water/polymer interface and additionally a structural roughness due to the head group COOH, which is ~3 Å thick

Table 2. Optimum Parameters To Describe the X-ray Reflectivity Curves Measured with the PFPE−COOH at the Points in the Isotherms Indicated (Lateral Pressure π; Molecular Area A)[a]

π (mN/m)	A (Å^2)	d (Å)	ρ (e$^-$/Å^3)	σ_{PA} (Å)	σ_{PW} (Å)	$V_{m,el}$ (Å^3)	$V_{m,d}$ (Å^3)
3.2	93.4	31.4 ± 1.0	0.506 ± 0.013	4.5 ± 0.6	2.8 ± 1.7	165.2 ± 4.1	134.4 ± 6.9
4.0	87.4	34.4 ± 1.2	0.496 ± 0.010	4.5 ± 0.6	3.3 ± 2.2	168.8 ± 4.1	138.1 ± 8.0
7.0	74.3	42.9 ± 1.2	0.513 ± 0.013	4.9 ± 0.9	2.6 ± 2.2	163.3 ± 4.1	146.3 ± 6.9
9.0	62.3	48.3 ± 1.6	0.466 ± 0.017	4.9 ± 0.9	1.6	179.4 ± 6.4	138.1 ± 7.3
15.0	55.4	54.5 ± 1.3	0.503 ± 0.013	5.5 ± 0.9	2.0	166.5 ± 4.1	138.5 ± 6.0
19.3	50.3	60.0 ± 1.4	0.519 ± 0.013	5.3 ± 0.9	2.8 ± 2.5	161 ± 4.1	138.5 ± 6.0
29.5	44.2	69.5 ± 1.2	0.536 ± 0.097	5.1 ± 0.8	4.3 ± 1.5	156 ± 28	140.8 ± 5.0

[a] Adjusted parameters are the film thickness d, its electron density ρ, the roughness σ_{PA} of the polymer/air interface, and σ_{PW}, the roughness of the polymer/water interface. $V_{m,el}$ is the volume per monomer unit as derived from the electron density (cf. eq 4), while $V_{m,d}$ was calculated from the film thickness d and the molecular area A (cf. eq 5). For comparison, $V_{m,bulk} = 156$ Å^3. The error was determined very conservatively, as described in the text. If it exceeds 100%, it is no longer quantified.

and thus of a similar size as the interfacial roughness σ_{PW}. Its electron density increases on compression—i.e., dehydratation—from ∼0.36 to ∼0.39 e$^-$/Å^3,[17] but the index of refraction is always intermediate between the one of the polymer and of the water. With this system it is very unlikely that the structural and the dynamic roughness can be distinguished, even if the system is chemically pure.

In contrast, the roughness at the polymer/air interface σ_{PA} is higher and constant, $\sigma_{PA} = 4.96 \pm 0.4$ Å. The deviation from the average value is even lower than the error bars of every single measurement. The good accuracy of σ_{PA} is obvious, if one evaluates eq 2a. The first two terms describe the average decay of the reflectivity curve; however, the very first term dominates, due to the large prefactor $\rho^2/\rho_w^2 = 2.3$ (compared to $(\rho - \rho_w)^2/\rho^2 \approx 0.27$). σ_{PA} describes the decay of the very first, numerically dominating term, and is thus determined with much better accuracy than σ_{PW}, which describes the decay of the small second term. Also, the range in Q is sufficient for a reliable measurement, for $Q = 0.35$/Å we obtain $\exp(-Q^2\sigma_{PA}^2) = 0.049$, a change of more than 1 order of magnitude. The interference term with the rather substantial prefactor $2(\rho/\rho_w)(\rho - \rho_w)/\rho_w \approx 2.2$ decays with the sum of the two roughnesses, $\rho_{PA} + \rho_{PW})^2$, and has thus no decisive influence.

It is intriguing to speculate on the origin of this constant roughness, which may be ascribed to capillary waves. The amplitude of a capillary wave at a fluid surface with the wavevector q is in a first approach determined by the surface tension γ.[18] The measured roughness is an average over all capillary wavevectors q, which can be "seen" by the detection system (capillary waves with $q < Q_{res}$ are not detected). For the measurable surface roughness, one obtains

$$\sigma_{AP}^2 = \frac{kT}{2\pi\gamma} \ln\left(\frac{q_{max}}{Q_{res}}\right) \tag{3}$$

Here, Q_{res} is the resolution of the setup, and q_{max} corresponds to the smallest wavelength of the capillary waves, which is determined by the molecular dimensions of the fluid. The static surface tension γ of the interface between air and bulk perfluoropolyether is 17 mN/m, and with our resolution, we expect to measure $\sigma_{PA} = 5.15$ Å, which agrees remarkably well with the observed value, $\sigma_{PA} = 4.96$ Å.

The surface tension at the water/polymer interface is assumed to be similar to the one between water and an isomeric polymer, i.e. $\gamma_o = 54.5$ mN/m;[19] this value yields a surface roughness of 2.9 Å. These values are about a factor of 2 smaller than the constant σ_{PA}, yet they are close to σ_{PW}, the roughness of the interface between water and bulk perfluoropolyether. However, considering the large error bars and the structural roughness, this may be just a coincidence.

If one assumes that, on the Langmuir trough, there is only one interface between water and air, one might deduce the interfacial roughness of this hypothetical interface from the overall surface tension γ using eq 3. One obtains a dynamical roughness of 2.6 Å at $\Pi = 0$, which increases on compression to 3.2 Å at $\Pi = 30$ mN/m (γ is determined with the Wilhelmy system: $\gamma = \gamma_o - \Pi$, with Π = lateral pressure and $\gamma_o = 72$ mN/m = surface tension of clean water).

However, the assumption of two interfaces is necessary for a satisfying description of the reflectivity data. These interfaces do not have the same roughness. The value determined for the upper interface $\sigma_{PA} = 4.96$ Å is in accordance with the surface tension of the interface between bulk perfluorether and air. It is, however, about a factor of 2 larger than the roughness of the lower interface or the roughness deduced by applying eq 3 to the surface tension on the trough.

At a film thickness of only 30 Å one might expect that coupling of both interfaces via the viscous polymer reduces the height of the amplitude of the capillary waves, which in turn would decrease the roughness σ_{PA}. The measured roughness, however, indicates a dynamic decoupling of the polymer/air interface from the polymer/water interface.

The constant electron density ρ of the monolayer indicates already that the film indeed has a constant volume. Yet, there are different ways to calculate ρ. To be certain that the results are self-consistent, the volume per polymer monomer unit V_m is calculated from the following:

(*i*) the electron density as determined from each measurement

$$V_{m,el} = N_e/\rho \tag{4}$$

(N_e is the number of electrons per monomer unit, in case of PFPE $N_e = 80$)

(*ii*) the product of molecular area per head group A and film thickness d divided by N, the average amount of monomer units per chain

$$V_{m,d} = Ad/N \tag{5}$$

(*iii*) the bulk density ρ_m as provided by the supplier, where m is the mass per monomer unit and N_A is Avogadro's constant

$$V_{m,bulk} = \rho_m N_A/m \tag{6}$$

This comparison is shown in Figure 4 as function of the area per head group. The volume per monomer unit found in the bulk phase (cf. eq 6), 154.8 Å^3, is rather

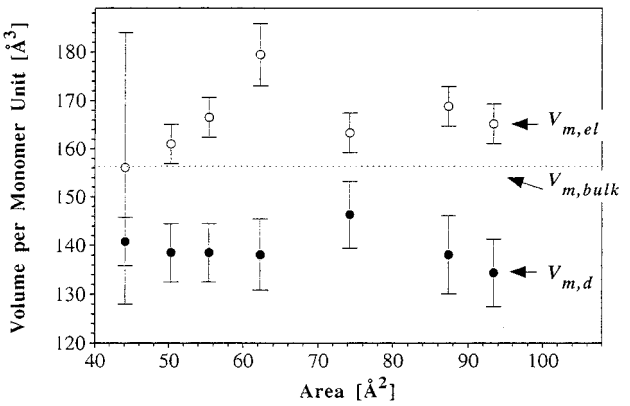

Figure 4. Volume per monomer unit of PFPE calculated from electron density (open symbols) and from film thickness and molecular area (filled symbols). The dotted line corresponds to the value measured in the bulk phase.

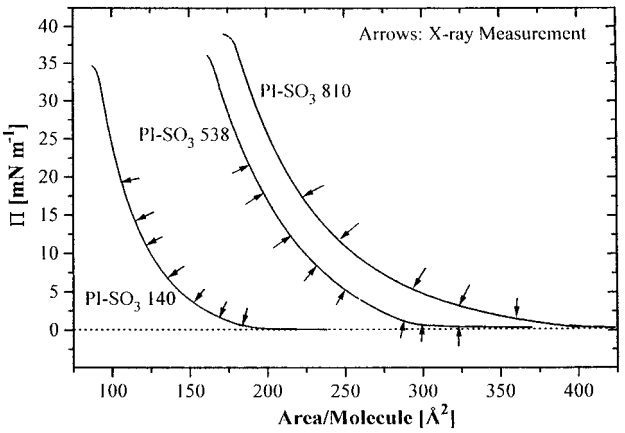

Figure 5. Isotherms of the different PI−SO_3-*N* investigated (T = 20 °C). Arrows indicate the points where X-ray reflectivity measurements were performed (cf. Table 3 and Figure 6). The change of slope at high pressures indicates a collapse of the film.

close to the one derived from the electron density, eq 4, 157.6 Å^3. This is a strong indication that a thin film which is only 30 Å thick exhibits already many properties of the bulk phase. Equation 5 is another independent way to calculate the volume per monomer unit directly from the X-ray reflectivity measurements; again, the result is remarkably constant, 138.6 Å^3, yet the numerical value is about 12% lower.

$V_{m,el}$ is calculated from the contrast of the X-rays reflected from the layered structure. However, the calculation of $V_{m,d}$ is based on the additional assumption that the *entire* material spread is in the homogeneous layer. Or in other words if $v_{m,d} < V_{m,bulk}$, the measured film thickness is less than that calculated from surface concentration and bulk density (as can be seen in Figure 8). Since 30% of the polymer does not have polar head groups, it is reasonable to assume that a fraction without head groups, has been lost during spreading and compression. This "lost" material does not necessarily have to leave the trough surface; it might as well retract into blobs of nonuniform height, which do not give rise to coherent interference. However no structure has been detected in Brewster angle microscopic images of the surface at pressures above 0 mN/m and below collapse of the film.[7] In the case of *complete* expulsion, we would expect an even thinner film thickness than experimentally determined. If the nonpolar terminated polymer is only partially expelled, one would expect further expulsion upon compression, and $V_{m,d}$ should not be independent of the area per head group (compare for example the swelling of phospholipid monolayers with alkanes[21]). It is therefore very likely that the fraction without polar head groups is not expelled from the polymer layer.

On the other hand, it is possible that the polymer contains a low molecular weight fraction that dissolves into the water subphase, as has been observed on monolayers of hydrophilically terminated poly(dimethylsiloxanes).[20]

In order to exclude these kind of effects it is therefore desirable to investigate polymer samples that have high purity and narrow molecular weight distribution. With the aim to verify and extend the somewhat tentative conclusions obtained with the PFPE−COOH, the polyisoprenes with sulfonate head groups listed in Table 1 were synthesized. The mass density of PI−SO_3 amounts to about half that of PFPE. The polymers are chromatographically pure and have a narrow molecular weight distribution. In order to investigate the theoretically predicted independence of the mass density on the chain length, the length of the tethered polymers was varied by a factor of almost 6. The isotherms depicted in Figure 5 are essentially as theoretically predicted, the longer the chain length the larger the entropically driven surface pressure. For each polymer, it is possible to vary the area per head group by a factor of 2.[8]

The polyisoprenes are better defined than the perfluoroethers; however, they appear to be affected by the X-ray beam: After about half an hour of exposure, the film appeared to thin while the pressure increased by up to 1 mN/m. This "thinning" was limited to the spot of irradiation. If a new spot was illuminated, the original thickness was observed. For a given chain length, this effect was more pronounced at large areas per molecule. The shortest polymer was the most stable. Presumably the radiation introduces additional polar groups to the polymer chain. This might happen either (i) due to the reaction of radiation damaged chain segments with the subphase or (ii) due to the reaction of the chain with radiolysis products formed in the water subphase. These additional polar groups may adsorb to the water subphase and cause an expansion of the damaged region.

To keep this effect to a minimum, for each measurement, a new film of tethered polyisoprene was prepared and measurements were completed within 20−30 min. The reflectivity curves (see Figure 6) show pronounced maxima. These maxima shift to lower Q values with decreasing area per molecule, similar to the PFPE shown in Figure 3; i.e., the film thickens on compression. For the different chain lengths we observe one to seven equidistant maxima. Furthermore, with increasing chain length, the extrema narrow; i.e., the thickness of the layer increases.

Note that for all measurements independent of area per molecule and chain length the contrast of the first maximum/minimum pair is almost identical, close to one, indicating that the electron density of the film is constant.

The theoretically expected contrast of this system is indeed about one, since the electron density of the bulk phase (ρ = 0.307 e$^-$/Å^3) is very similar to that of the subphase (ρ_w = 0.333 e$^-$/Å^3). The two terms describing the contrast exhibit a small and a tiny prefactor, i.e. $\rho^2/\rho_w^2 \approx 0.85$ and $(\rho - \rho_w)^2/\rho_w^2 \approx 0.006$. The prefactor

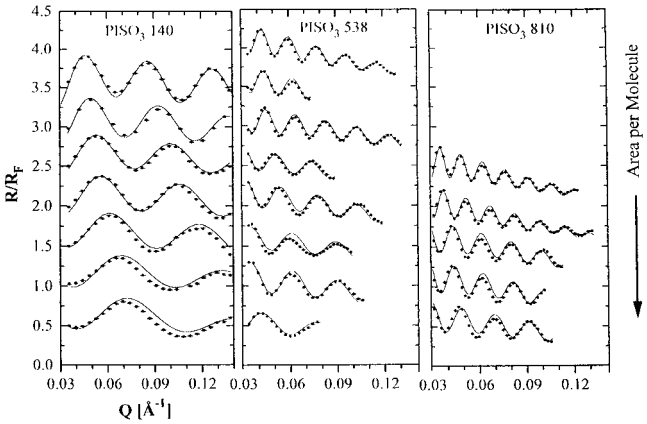

Figure 6. Normalized X-ray reflectivity curves measured with PI−SO_3-*N* at the molecular areas indicated in Figure 5. The measured X-ray intensities are given together with their statistical error bars; the solid lines are simulations with the optimized parameters given in Table 3. For clarity, each measurement is displaced vertically by 1 unit from the next.

Table 3. Optimum Parameters To Describe the X-ray Reflectivity Curves Measured with the Polyisoprenes (a) PI−SO_3-140, (b) PI−SO_3-538 and (c) PI−SO_3-810[a]

PI−SO_3-140

π (mN/m)	A (Å^2)	d (Å)	ρ (e$^-$/Å^3)	σ_{PA} (Å)	σ_{PW} (Å)	$V_{m,el}$ (Å^3)	$V_{m,d}$ (Å^3)
0.5	184.3	87.8	0.299	4.6	7.1	127.1	115.6
1.6	166.0	93.6	0.303	3.9	6.5	125.5	111.0
3.5	152.8	106.5	0.305	4.2	0.5	134.7	116.2
6.8	136.7	119.5	0.298	3.8	3.4	127.5	116.7
11.0	122.8	126.7	0.300	3.9	5.6	126.7	111.1
14.4	116.3	143.8	0.294	3.8	3.8	129.1	119.4
19.0	108.2	149.8	0.292	4.0	2.9	130.0	115.8

PI−SO_3-538

π (mN/m)	A (Å^2)	d (Å)	ρ (e$^-$/Å^3)	σ (Å)	$V_{m,el}$ (Å^3)	$V_{m,d}$ (Å^3)
0.5	325.6	166	0.313	7.1	121.4	106.5
0.7	298.9	216	0.304	6.7	125.1	119.8
1.2	287.8	226	0.313	6.5	121.4	120.9
5.2	250.0	267	0.310	6.9	122.5	124.1
8.3	232.2	274	0.308	8.2	123.2	118.2
12.3	215.5	313	0.306	6.7	124.0	125.4
17.8	197.8	327	0.303	10.3	125.5	120.2
21.5	188.9	346	0.305	9.1	124.7	121.5

PI−SO_3-810

π (mN/m)	A (Å^2)	d (Å)	ρ (e$^-$/Å^3)	σ (Å)	$V_{m,el}$ (Å^3)	$V_{m,d}$ (Å^3)
1.5	360.0	283.7	0.308	6.7	123.2	126.1
3.0	322.2	320.2	0.305	8.1	124.7	127.4
6.0	294.4	324.5	0.306	8.0	124.4	117.9
12.5	247.8	393.5	0.303	9.7	125.5	120.4
16.0	222.2	425.4	0.299	11.0	127.1	116.7

[a] The (π,*A*)-points at the isotherm are given in the first column. The optimized parameters are the same as for Table 2, yet for the two longer polymers a single interfacial roughness parameter σ is sufficient to describe the data. For comparison, $V_{m,bulk}$ = 123.7 Å.

of the interference term is not very large, either $(2(\rho/\rho_w)(\rho - \rho_w)/\rho_w \approx 0.16)$.

Mainly, the short measurement times do limit the accessible *Q* range; also, the signal to noise ratio is not as good as it could be. The thinner the film is, the less minima and maxima are in the accessible *Q* range, leading to larger uncertainities in the data analysis. Therefore, the data derived from the shortest polymer are the least reliable. Theoretically, the SO_3^- group has a higher electron density than both the film and the water, yet we cannot resolve it. Also, the question of the dynamic decoupling of the polymer/air interface and the water/polymer interface cannot be addressed meaningfully due to the small accessible range in *Q* and the chemical instability.

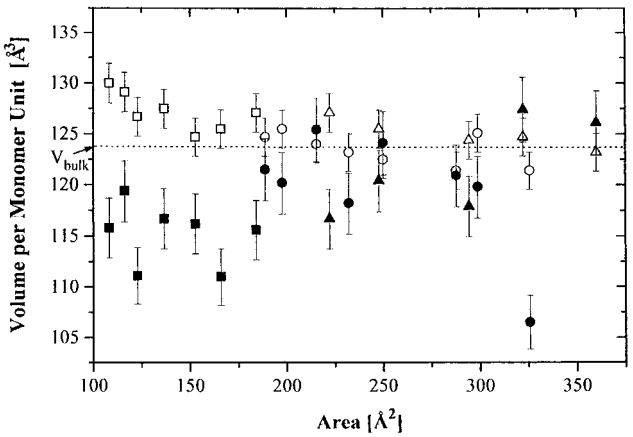

Figure 7. Volume per repeat unit of a polyisoprene chain calculated from electron density (open symbols) and from film thickness and molecular area (filled symbols). The straight line corresponds to the value measured in the bulk phase. Squares symbolize measurements of PI−SO_3-140, circles of PI−SO_3-538, and triangles of PI−SO_3-810.

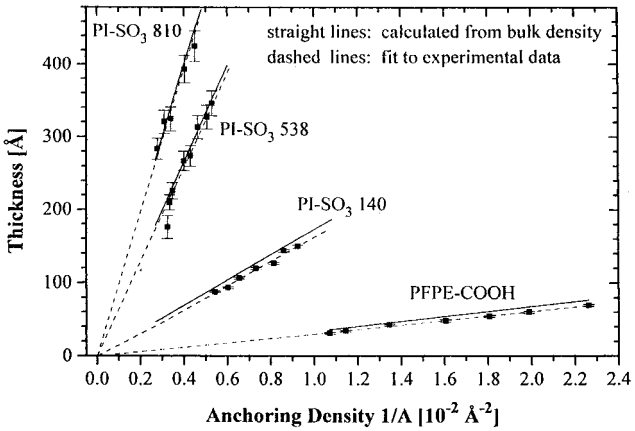

Figure 8. Film thickness *d* as a function of the anchoring density 1/*A*, which is defined as the inverse area per head group. Points indicate measurements; the dotted lines are best linear fits assuming a linear dependce. The solid lines were calculated from the anchoring density assuming the bulk density, and the nominal degree of polymerization.

Since the polymer films are rather thick, it is possible to simulate the data with the one-slab model used before, even if the range in *Q* is rather small. The results are given in Table 3 and Figure 7. Again, the volume per monomer unit calculated either from the electron density or from the product of molecular area and film thickness gives very self-consistent results. The numerical values obtained by the two methods agree very well, with the volume per monomer as found in the bulk polymer intermediate. The worst deviations occur with the thinnest polymer. To analyze these measurements one has to go further in *Q* to obtain a few extrema; i.e., one has to measure longer. Thus the deviation is witness to the chemical decomposition. Quantitatively, the agreement (3% deviation from the bulk value) is better than that with the PFPE (12%).

The roughnesses are fudge parameters, largely dependent on the chosen range in *Q* and presumably influenced by the chemical degradation. Generally, the values are too large to be explained with eq 3 and the

surface tension measured with the Wilhelmy system.

The very good agreement obtained for the different methods to calculate the volume per monomer unit demonstrates the validity of the assumption of constant volume. The constant volume per monomer unit implies a linear dependency of the film thickness as function of the anchoring density $1/A$, which is indeed found, as Figure 8 shows. The PI−SO_3's are longer than the PFPE; thus, the films are thicker, between 90 and 420 Å. While one observes the expected linear increase of the film thickness with the anchoring density, the film thicknesses are a bit lower than expected. In the case of PFPE, this is presumably due to the loss of material, while chemical degradation is the problem of the PI−SO_3's.

Conclusion

Hydrophobic polymers with a low glass transition temperature and a ionic head group form stable monolayers on the water surface. We can regard these monolayers qualitatively as polymer brushes of a polymer melt of constant volume tethered to a planar interface, yet if a feasible percentage of the head groups lose their anchoring, the electron density does not change much. This was shown for chain lengths consisting of between 66 and 3200 C atoms; for each polymer the anchoring density and thus the film thickness were varied within a factor of 2. These results are valid for films thicker than 30 Å. The dynamic properties of the films are still not very well understood. The data suggest that capillary waves at the polymer/air interface cause an increased roughness; thus, the polymer/air interface would be independent of the dynamic properties of the anchoring interface, which has a lower roughness.

Acknowledgment. We enjoyed stimulating discussions with H. Möhwald and M. Antonietti. The hospitality of M. Schmidt, in whose laboratory some of these measurements were performed, is appreciated. We thank J. Linn, G. B. Street, G. Vurens and J. Burns for providing PFPE−COOH along with the characterization data; S. Förster for vital discussions concerning the anionic polymerization; G. Czichocki, A. Martins and P. Müller for analytical and preparative HPLC. We are grateful to the Deutsche Forschungsgemeinschaft (Mö 283/31-1, Gö 693/1-1,2), the SFB 262, and the Max-Planck-Society for financial support.

References and Notes

(1) Alexander, S. *J. Phys.* **1977**, *38*, 983.
(2) Gennes, P.-G. de *Macromolecules* **1980**, *13*, 1069.
(3) Halperin, A.; Tirrell, M.; Lodge, T. P. *Adv. Polym. Sci.* **1992**, *100*, 31.
(4) Semenov, A. N. *Sov. Phys. JETP* **1985**, *61*, 733.
(5) Semenov, A. N. *Macromolecules* **1993**, *26*, 6617.
(6) Lenk, T. J.: Lee, D. H. T.; Koberstein, J. T. *Langmuir* **1994**, *10*, 1857.
(7) Goedel, W. A.; Xu, C.; Frank, C. W. *Langmuir* **1993**, *9*, 1184. Goedel, W. A.; Wu, W. A.; Friedenberg, M. C.; Fuller, G. G.; Foster, M.; Frank, C. W. *Langmuir* **1994**, *10*, 4209−4218.
(8) Heger, R.; Goedel, W. A. *Macromolecules* **1996**, *29*, 8912.
(9) Ulman, A. *An Introduction to Ultrathin Organic Films: From Langmuir-Blodgett to Self-Assembly*; Academic Press: Boston, MA, 1991.
(10) Mirley, C. L.; Koberstein, J. T. *Langmuir* **1995**, *11*, 1049.
(11) Lowack, K.; Helm, C. A. *Adv. Mater.* **1995**, *7*, 155.
(12) Als-Nielsen, J. In *Structure and Dynamics of Surfaces*; Blanckenhagen, W. S. a. W., Ed.; Springer: New York, 1986.
(13) Helm, C. A.; Möhwald, H.; Kjaer, K.; Als-Nielsen, J. *Europhys. Lett.* **1987**, *4*, 697.
(14) Baltes, H.; Schwendler, M.; Helm, C. A.; Möhwald, H. *J. Colloid Interface Sci.* **1996**, *178*, 135.
(15) Press, W. H.; Flannery, B. P.; Teukolsky, S. A.; Vetterling, W. T. *Numerical Recipes in Pascal*; Cambridge University Press: Cambridge, England, 1989.
(16) Baltes, H.; Schwendler, M.; Helm, C. A.; Möhwald, H.; Struth, B.; Scalas, E.; Brezesinski, G. In *Short and Long Chains at Interfaces, Proceeding of the XXXth Rencontres de Moriond*; Daillant, J., Guenoun, P., Marques, C., Muller, P., Vân, J. T. T., Eds.; Editions Frontières, Gif-sur-Yvette, France, 1996.
(17) Kjaer, K.; Als-Nielsen, J.; Helm, C. A.; Tippmann-Krayer, P.; Möhwald, H. *J. Phys. Chem.* **1989**, *93*, 3200.
(18) Schwartz, D. K.; Schlossman, M. L.; Kawamoto, E. H.; Kellogg, G. J.; Pershan, P. S. *Phys. Rev. A* **1990**, *41*, 5687.
(19) Bernelt, M. K.; Zisman, W. A. *J. Phys. Chem.* **1973**, *77*, 2324.
(20) Elman, J.-F.; Lee, D. H. T.; Thompson, P. M.; Koberstein, J. T. *Langmuir* **1995**, *11*, 2761.
(21) Thoma, M.; Schwendler, M.; Baltes, H.; Helm, C. A.; Pfohl, T.; Riegler, H.; Möhwald, H. *Langmuir* **1996**, *12*, 1722.

MA970232R